

Potential new opportunities utilizing lab facilities for elucidating the fundamental plasma physics mechanisms at play in space plasmas

M.E. Koepke, *West Virginia University*

with valuable input from

Jim Bailey (*Sandia*),

Chris Chaston (*UC-Berkeley*),

Herbert Gunell (*Belgian Inst. Space Aeronomy, Belgium*),

David Knudsen (*Univ Calgary*),

Thomas Leyser (*Uppsala Univ., Sweden*),

Richard Marchand (*Univ Alberta*), and

Hans Pécseli (*Univ Oslo*)

Principles of Interrelationship between Plasma Experiments in the Laboratory and in Space

The premise of investigating basic plasma phenomena relevant to space is that an alliance exists between both basic plasma physicists, using theory, computer modelling and lab experiments, and space scientists, using different instruments, either flown on different spacecraft in various orbits or stationed on the ground.

Dedicated lab-studies (1) probe and elucidate fundamental plasma physical processes, (2) provide benchmarks for validating theory and modeling, and (3) produce spectroscopic measurements, all in support of interpreting rocket, satellite and telescope data.

Facilitating this interaction is diagnostic development, emerging instrumentation, and advanced scientific research in computer modeling and simulation.

Campaign Models of IPELS:

Examples from the scientific community

BaPSF Space Plasma Campaign (UCLA-LAPD)

- Stationary Inertial Alfvén Wave

Center for Magnetic Self-Organization

in Laboratory and Astrophysical Plasmas (Univ Wisc-CMSO)

- Dynamo – Magnetic Reconnection – Magnetic Helicity Conservation and Transport – Angular Momentum Transport – Ion Heating – Magnetic Chaos and Transport

Z Astrophysical Plasma Properties (Sandia National Lab – Z)

- Solar-Interior Opacity – White Dwarf – Black Hole Accretion Disk – Active Galactic Nucleus

Lab Astrophysics at NIF (Lawrence Livermore National Lab)

- Evolution of unstable interface when heated by a shock in a supernova explosion
- Rayleigh-Taylor hydrodynamic instabilities during dying star's core collapse – Planetary physics
- Nuclear astrophysics – Radiative transfer – Lab production of relativistic electron-positron pair plasmas (γ -ray bursts, black holes, AGN, early universe, pulsar magnetosphere)

International Space Science Institute (Bern, Switzerland)

- Contribute to deeper understanding of results from different space missions, ground based observations and lab experiments. Add value to results through multidisciplinary research, International Teams, Workshops, Working Groups, Forums or as individual Visiting Scientists.

Multidisciplinary University Research Initiative (Univ Md, Air Force MURI)

- Fundamental physics issues on radiation belts and remediation: radiate, propagate, amplify, precipitate

Scaling: Challenges and Successes

TABLE 1. Space Parameters^a

	Interstellar Medium	Heliosphere	Solar Wind	Magnetosphere		Ionosphere	
				Magnetopause	Inside Boundary Layer	F Region	E Region
n, cm^{-3}	0.1–10	0.01–1	5–60	20	1	10	10
$k_B T_i, \text{eV}$	0.5–1	0.1–10	1–50	800	4000	0.15	0.05
B	0.1–50 μG	1–10 μG	10–200 μG	250 μG	400 μG	0.3 G	0.3 G
β	1	1	1	10	1	10	10
ω_{pe}/ω_{ce}	300	200	100	50	15	1	0.1
ω_{pi}/ω_{ci}	10,000	10,000	5,000	2,500	300	200	50
Ion gyroradius	100 km	200 km	50 km	140 km	160 km	1 m	1 m
Debye length	10 m	1 m	10 m	50 m	500 m	1 cm	1 cm

^aLaboratory and space values of n , T , and some other parameters are not comparable. See *Eastman* [1990].

TABLE 3. Parameter-Value Comparison From *Bamber et al.* [1995]

	Ionosphere	Laboratory
f/f_{LH}	1–7	6.7
f/f_{ce}	0.005–0.03	0.077
f_{pe}/f_{ce}	0.6–1.0	6.5
d/ρ_{ci}	2–150	15
d/L_{∇}	1–10	4.6
$\lambda_{\parallel}/L_{\nabla}$	2–650	12.3
$\lambda_{\perp, LH}/L_{\nabla}$	0.1–3.5	1.1
k_{\parallel}/k_{\perp}	0.003–0.07	0.091

TABLE 4. Parameter-Value Comparison From *Koepke et al.* [1999]

	Ionosphere	Laboratory
f/f_{ci}	0.1–4	0.3–5
k_{\parallel}/k_{\perp}	<0.22	0.02–2
$f\lambda_{\parallel}/\langle v_{ze} \rangle$	0.9	<1.0
$f\lambda_{\perp}/v_{Ti}$	1	1
f_{pe}/f_{ce}	0.6 – 1.0	0.1
f_{pi}/f_{ci}	200	40

Koepke, Interrelated lab and space plasma experiments, *Rev. Geophys.* 46, RG3001 (2008).

Scaled laboratory experiments explain the kink behaviour of the Crab Nebula jet

C.K. Li, P. Tzeferacos, D. Lamb, G. Gregori, P.A. Norreys, M.J. Rosenberg, R.K. Follett, D.H. Froula, M. Koenig, F.H. Seguin, J.A. Frenje, H.G. Rinderknecht, H. Sio, A.B. Zylstra, R.D. Petrasso, P.A. Amendt, H.S. Park, B.A. Remington, D.D. Ryutov, S.C. Wilks, R. Betti, A. Frank, S.X. Hu, T.C. Sangster, P. Hartigan, R.P. Drake, C.C. Kuranz, S.V. Lebedev & N.C. Woolsey, *NATURE COMMUNICATIONS* 7, 13081 (2016).

The remarkable discovery by the Chandra X-ray observatory that the Crab nebula's jet periodically changes direction provides a challenge to our understanding of astrophysical jet dynamics. It has been suggested that this phenomenon may be the consequence of magnetic fields and MHD instabilities, but experimental demonstration in a controlled laboratory environment has remained elusive.

Experiments are reported that use high-power lasers to create a plasma jet that can be directly compared with the Crab jet through well-defined physical scaling laws. The jet generates its own embedded toroidal magnetic fields; as it moves, plasma instabilities result in multiple deflections of the propagation direction, mimicking the kink behaviour of the Crab jet. The experiment is modelled with three-dimensional numerical simulations that show exactly how the instability develops and results in changes of direction of the jet.

Scaled laboratory experiments explain the kink behaviour of the Crab Nebula jet

Table 1 | Physical parameters and similarity scaling between the laboratory jet and the Crab nebula jet.

Parameters and scales	Plasma jet in OMEGA experiment*	Scaled to the Crab nebula†	The kinked jet in the Crab nebula†
Temperature	T_e	~ 300 eV	~ 1 -130 eV
Ionization state	Z	~ 3.5	~ 1
Number density	n_e	$\sim 5 \times 10^{19} \text{ cm}^{-3}$	$\sim 10^{-2} \text{ cm}^{-3}$
Pressure	P	$\sim 4 \times 10^5$ bar	$\sim 4 \times 10^{-14}$ bar
Jet radius	r_j	$\sim 5 \times 10^{-2}$ cm	~ 1 pc
Jet velocity	v_j	$\sim 400 \text{ km s}^{-1}$	$\sim 1.2 \times 10^5 \text{ km s}^{-1}$
Time scale	τ	$\sim 10^{-9}$ s	$\sim \text{few years}$
Magnetic field	B	~ 2 MG	~ 1 mG
Thermal plasma beta	β	~ 0.1 -1	$\ll 1$
Magnetization parameter	σ	~ 1 -6	≥ 1
Mach number	M	~ 3	$\gg 1$
Reynolds number	Re	$\sim 2 \times 10^3$	$\sim 2 \times 10^{17}$
Péclet number	Pe	~ 1 -5	$\sim 4 \times 10^{15}$
Magnetic Reynolds number	Re_M	$\sim 3 \times 10^3$	$\sim 1 \times 10^{22}$
Biermann number	Bi	~ 6	$\sim 6 \times 10^8$
Radiation number	Π	$\sim 3 \times 10^5$	$\sim 1 \times 10^{18}$

*Near the region of jet launching.

†Near the region of the pulsar pole.

The bold entries show the physical quantities from the two systems that can be directly compared through the scalings in equations (3), manifesting how the laboratory experiment parameters scale to match those of the Crab nebula jet.

$$\begin{aligned}
 r_{\text{lab}} &= ar_{\text{crab}}; & \rho_{\text{lab}} &= b\rho_{\text{crab}}; & P_{\text{lab}} &= cP_{\text{crab}}; \\
 v_{\text{lab}} &= \sqrt{\frac{c}{b}}v_{\text{crab}}; & \tau_{\text{lab}} &= a\sqrt{\frac{b}{c}}\tau_{\text{crab}}; & \mathbf{B}_{\text{lab}} &= \sqrt{c}\mathbf{B}_{\text{crab}},
 \end{aligned} \tag{3}$$

where the subscripts ‘lab’ and ‘crab’ refer to the laboratory and Crab nebula jets, respectively. As shown in Table 1, excellent MHD scaling is obtained with $a \sim 1.6 \times 10^{-20}$, $b \sim 1.7 \times 10^{25}$ and $c \sim 1.1 \times 10^{19}$.

Scaled laboratory experiments explain the kink behaviour of the Crab Nebula jet

Other evidence of the relevance of our experiments to the jet in the Crab nebula is provided by several important dimensionless parameters. Both jets have a Lorentz factor of the order of unity ($\Gamma = 1$ for the laboratory plasma jet and $\Gamma \approx 1.09$ for the Crab Nebula jet³⁰). Similarity in the MHD equations requires that the dissipative processes be negligible for both systems. This requirement is met if the viscosity, thermal conduction, and magnetic diffusion terms can be neglected in the momentum, energy, and generalized Ohm's law equations. Equivalently, a number of corresponding dimensionless numbers, such as the Reynolds number $Re(=Lv_j/\nu$, the ratio of inertial forces to viscous force, where L is jet scale size and ν is the kinematic viscosity), the Péclet number $Pe(=Lv_j/\kappa$, the ratio of heat convection to conduction, where κ is the thermal diffusivity), and the magnetic Reynolds number $R_{Me}(=Lv_j/D_m$, the ratio of flow velocity to diffusion velocity, where D_m is the magnetic diffusivity) must be large in both systems. Table 1 shows that all of these numbers are large, demonstrating that these important conditions are met. Table 1 also lists the other physical parameters and dimensionless numbers that are relevant to this laboratory jet and to the jet in the Crab nebula. To scale the laboratory results to the environment of the Crab nebula, the MHD equations need to be invariant under the transformations given below for the two systems^{17,18}:

ABSTRACT for this talk

Suggestions for space plasma physics campaigns to be carried out on current and forthcoming experimental facilities were solicited from space scientists passionate about the interrelationship between plasma experiments in the laboratory and in space. The received ideas will be outlined in terms of realizable configurations.

Examples of realizable ideas

- Systematic study of the transition from weak to strong turbulence of low frequency fluctuations in magnetized plasmas [[H. Pécseli](#)];
- Investigation of the localized electrostatic turbulence inside neighboring striations and the electromagnetic coupling between these different striations and/or the turbulence inside them [[T. Leyser](#)]
- Re-creating the conditions of a electrostatic, i.e., inverted V, aurora to verify the theory for auroral particle acceleration [[H. Gunell](#)].
- Collaborate on NASA small-explorer missions [[C. Chaston](#)]
- Alfvén wave physics [[D. Knudsen](#)]
- Whole-device modeling [[R. Marchand](#)]
- At-parameter experimental astrophysics [[J. Bailey and ZAPP](#)]

Systematic study of the transition from weak to strong turbulence of low frequency fluctuations in magnetized plasmas

H. Pécseli, University of Oslo, Oslo, Norway

The resistive drift wave is one possibility but this only specifies the basic instability. In general there are several other candidates/possibilities. This could be a nice combination of theoretical, experimental (laboratory and space observations) and numerical methods.

“Spectral properties of electrostatic drift wave turbulence in the lab and the ionosphere”, H.L. Pécseli, *ANNALES GEOPHYSICAE* 33, 875-900 (2015) suggests a systematic study of spectral shapes, in the hope they reveal universal features relating to weak/strong turbulence conditions.

Low Frequency Waves and Turbulence in Magnetized Laboratory Plasmas and in the Ionosphere, H.L. Pécseli, Copyright © IOP Publishing Ltd 2016
Online ISBN: 978-0-7503-1251-6 • Print ISBN: 978-0-7503-1252-3

Investigation of the localized ES turbulence inside several, neighboring, EM-coupled, strongly-inhomogeneous-turbulence-containing striations

T. Leyser, Uppsala University, Uppsala, Sweden

“Several striations interacting” is a unique configuration possible in UCLA’s LAPD and ETPD. The relationship(s) between local plasma processes, including strongly inhomogeneous turbulence, and global-scale response of the plasma, could be documented over widely different spatial scales, specifically electrostatic and electromagnetic scales, and related to ionospheric HF-pumping of ionospheric plasma.

Little theory exists. Simulations are sparse. We lack measurements, without which real progress is difficult.

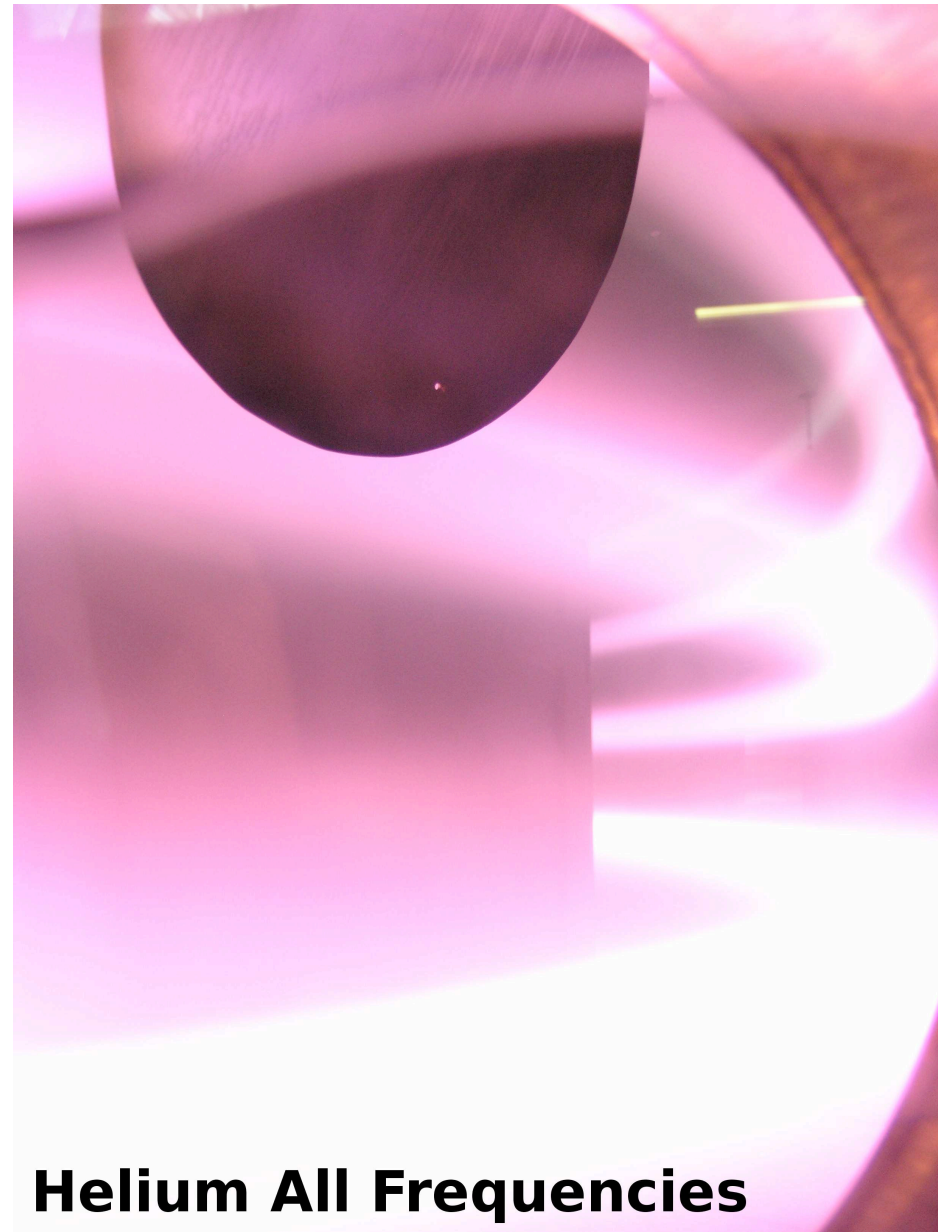
The problem additionally involves a wide range of temporal scales (diffusive and ponderomotive processes together).

Lab striations: Flux ropes and ETPD multi-rings

The link to a recent special issue on flux rope physics:

iopscience.iop.org/issue/0741-3335/56/6;jsessionid=D356C8A2559E41FA520C0CE005EDEA97.ip-10-40-1-105

Enormous Toroidal Plasma Device
UCLA-BaPSF →



Helium All Frequencies

Re-creating the conditions of a electrostatic aurora to verify auroral particle acceleration theory

H. Gunell, Belgian Institute for Space Aeronomy, Brussels, Belgium

Build an aurora simulation device to re-create the conditions of a electrostatic, i.e., inverted V, aurora. Cold ionospheric plasma is provided by Q-machine source on one end and hot magnetospheric electrons are provided by discharge at other end.

Numerical and laboratory simulations of auroral acceleration, H. Gunell, J. De Keyser, and I. Mann, *Physics of Plasmas* 20, 102901 (2013);

Can the downward current region of the aurora be simulated in the laboratory?, H Gunell, L Andersson, J De Keyser, and I Mann, *Plasma Phys. Control. Fusion* 58 054003 (2016).

With such a device one would be able to access the low-voltage regime that is difficult to simulate numerically.

Perpendicular heating mechanisms would be included naturally in the lab device and, so far, these have not been modelled self-consistently in computer simulations.

Search for the conditions and signatures of electromagnetic aurorae

H. Gunell, Belgian Institute for Space Aeronomy, Brussels, Belgium

Alfvénic auroras exist, as both electrostatic and Alfvénic aspects of the aurora may be present at the same time.

Configuring the LAPD to have a mirror field and a Q-machine source could generate the necessary Alfvén waves.

Shocks and boundary layers

H. Gunell, Belgian Institute for Space Aeronomy, Brussels, Belgium

Bow shocks and magnetopauses exist at Earth and the other planets. Similar boundaries exist at comets and at the boundary of the diamagnetic cavity.

MHD and hybrid simulations have been used to model such boundaries on large scales, but these models all use simplifying assumptions, and the details of the kinetic physics and smaller scale phenomena are not included.

With the MMS spacecraft now flying, we shall learn a lot more about Earth's bow shock: the physics of the foreshock region, the formation of short large-amplitude magnetic structures (SLAMS) and plasmoids, currents at the bow shock, the voltage across it, and other features.

Collaborate on NASA small-explorer missions

C. Chaston, Univ California – Berkeley, CA

A parallel lab experiment can benefit parent mission.

Mission science often lends itself nicely to lab work.

Explorers Missions:

Investigations characterized by maximum allowed total cost to NASA for definition, development, mission operations, and data analysis.

Medium-Class Explorers (MIDEX): Costs not to exceed \$180 to \$200 million.

Missions in Development — ICON | TESS Operational Missions — ACE | Swift | THEMIS
Past Missions — FUSE | IMAGE | RXTE (XTE) | WISE | WMAP (MAP)

Small Explorers (SMEX): Costs not to exceed \$120 million.

Missions in Development — IXPE Op Missions — AIM, IBEX, IRIS, NuSTAR, RHESSI (HESSI)
Past Missions — FAST | GALEX | SAMPEX | SWAS | TRACE

University-Class Explorers (UNEX): Costs not to exceed \$15.0 million.

Past Missions — CHIPS | SNOE

Missions of Opportunity (MO): Having a total NASA cost of under \$55 million

Investigations characterized by being part of a non-NASA space mission of any size.

These missions are conducted on a no-exchange-of-funds basis with the sponsoring organization.

NASA intends to solicit proposals for Missions of Opportunity with each

Announcement of Opportunity (AO) issued for EX, UNEX, SMEX, and MIDEX investigations.

Missions in Development — GOLD | NICER Operational Missions — TWINS
Past Missions — CINDI | HETE-2 | Hitomi (ASTRO-H) | Suzaku (Astro-E2)

Internationals

Operational Missions — INTEGRAL

Alfvén wave physics

D. Knudsen, University of Calgary, Canada

The Science: Auroral electron acceleration, from Alfvén-wave-induced formation of a parallel electric field and the consequent current-carrying population of energetic particles (particles with energies well above the typical ‘thermal’ energy of the system), is a key dynamic in the magnetosphere-ionosphere coupling in geospace.

Alfvén wave physics

D. Knudsen, University of Calgary, Canada

Outcome: Azimuthal convective flow and density-depleted magnetic- field-aligned current, co-located in the helium plasma produced in the large plasma device (LAPD-U) at UCLA, support an Alfvénic perturbation that is static in the lab frame.

Electrostatic probes measure the flow and static density perturbations in the 72 cm-diameter, 12 m-long, afterglow plasma, wherein a radially segmented electrode creates the convective flow and an off-cylindrical-axis planar-mesh electrode draws current in a channel parallel to the background magnetic field.

This stationary ‘wave’ is measured as a fixed (in the lab frame) ion density structure.

Alfvén wave physics

D. Knudsen, University of Calgary, Canada

The Impact: Time-stationary, self-excited, magnetized-plasma structure that arises in the perturbed plasma quantities is measured in the laboratory when a channel of magnetic-field-aligned (parallel) electron current and associated density depletion are co-located with cross-field plasma convection ($E \times B$ flow).

These ingredients are responsible for lab evidence for the existence of StIA wave and are being employed with the intention to validate stationary inertial Alfvén wave (StIAW) theory in the laboratory.

Laboratory evidence for stationary inertial Alfvén waves and its relevance to auroral plasma, ME Koepke, SH Nogami, SM Finnegan, S Vincena, DJ Knudsen, DM Gillies, M Tornquist, D Vassiliadis, PPCF 58, 084006 (2016).

Whole-device modeling

R. Marchand, University of Alberta, Canada

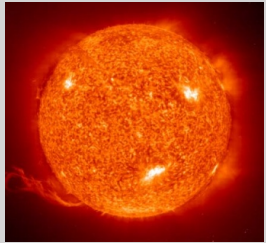
The basic idea is not to rely on idealized theories to interpret probe, and more generally particle sensor, measurements, but to rely on a simulation that has been fit to raw (unprocessed) measurements made with sensors that were "optimally positioned" around a volume of interest.

Fit simulation results to local (at sensors) measurements, instead of to plasma parameters derived by translating sensor data first into local measurements using conventional diagnostic theory.

At-parameter experimental astrophysics

J. Bailey + ZAPP collaboration, Sandia National Labs, Albuquerque, NM

Solar Opacity



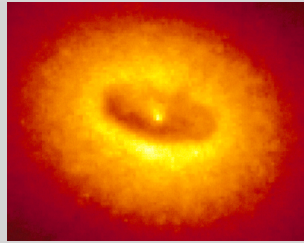
Goal: Predict the location of the convection zone boundary in the Sun.

Achieved Conditions:

$T_e \sim 200 \text{ eV}$
 $n_e \sim 10^{23} \text{ cm}^{-3}$



Photoionized Plasma



Goal: Predict ionization and line formation occur in accreting objects.

Achieved Conditions:

$T_e \sim 20 \text{ eV}$
 $n_e \sim 10^{18} \text{ cm}^{-3}$



White Dwarf Lineshape



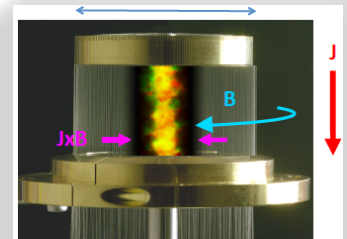
Goal: Predict correct properties for White Dwarfs by improved spectral fitting.

Achieved Conditions:

$T_e \sim 1 \text{ eV}$
 $n_e \sim 10^{17} \text{ cm}^{-3}$



Stark Broadening



Goal: Differentiate single- and multiple-element Stark broadened spectra.

Achieved Conditions:

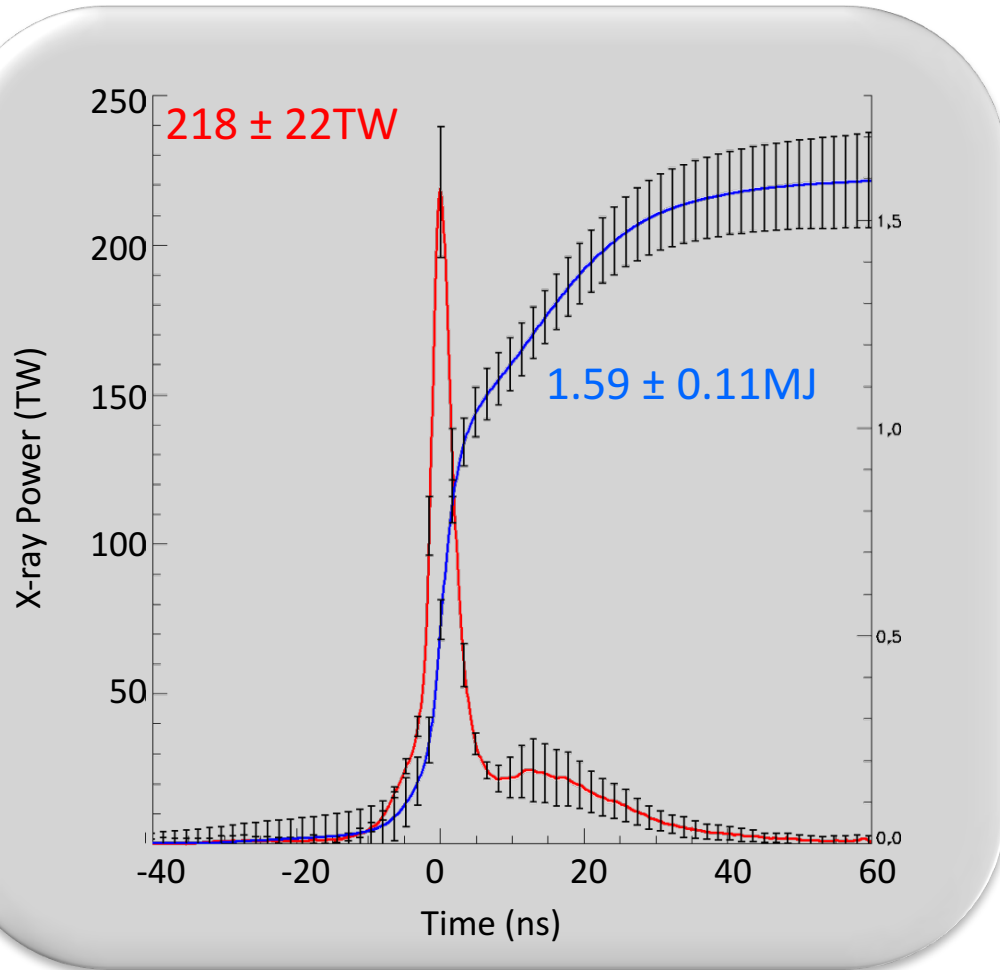
$T_e \sim 60 \text{ eV}$
 $n_e \sim 2 \times 10^{21} \text{ cm}^{-3}$



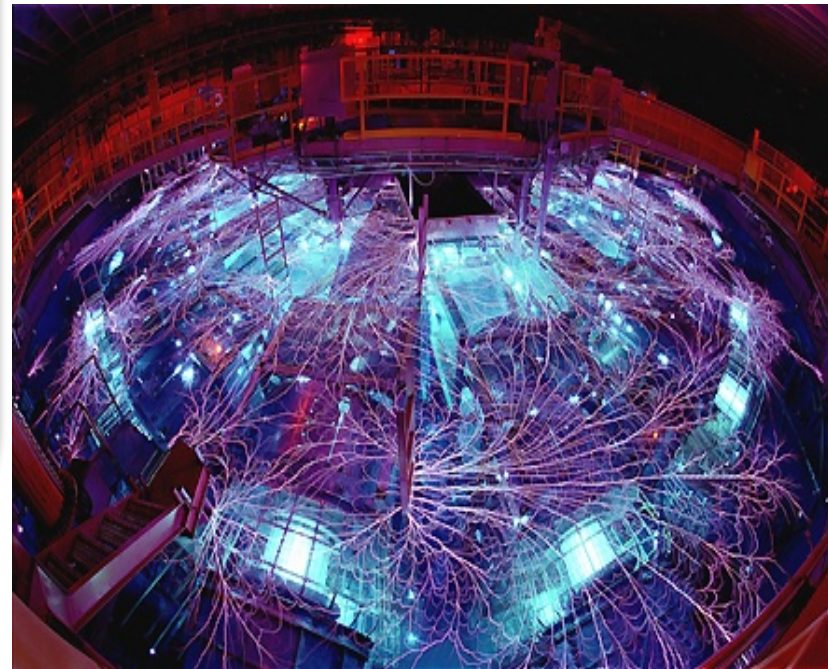
Campaigns study issues spanning 200x in T and 10^6 in n_e

Hohlraum x-ray emission reproducibly heats for 100ns and backlights for 3ns.

Radial X-ray Power and Energy (20-shot avg)



	ZR >2011	Z <2007
Marx Energy	20.3 MJ	11.4 MJ
I _{peak}	25.8 MA (1.5%)	21.7 MA* (2.1%)
Mass	8.5 mg	3.8 mg
Peak Power	220 TW (10%)	120 TW (14%)
Radiated Energy	1.6 MJ (7%)	0.82 MJ (17%)



Dynamic hohlraum produces tungsten plasma that implodes low-density CH₂ foam, launches shock, radiates x-rays outward

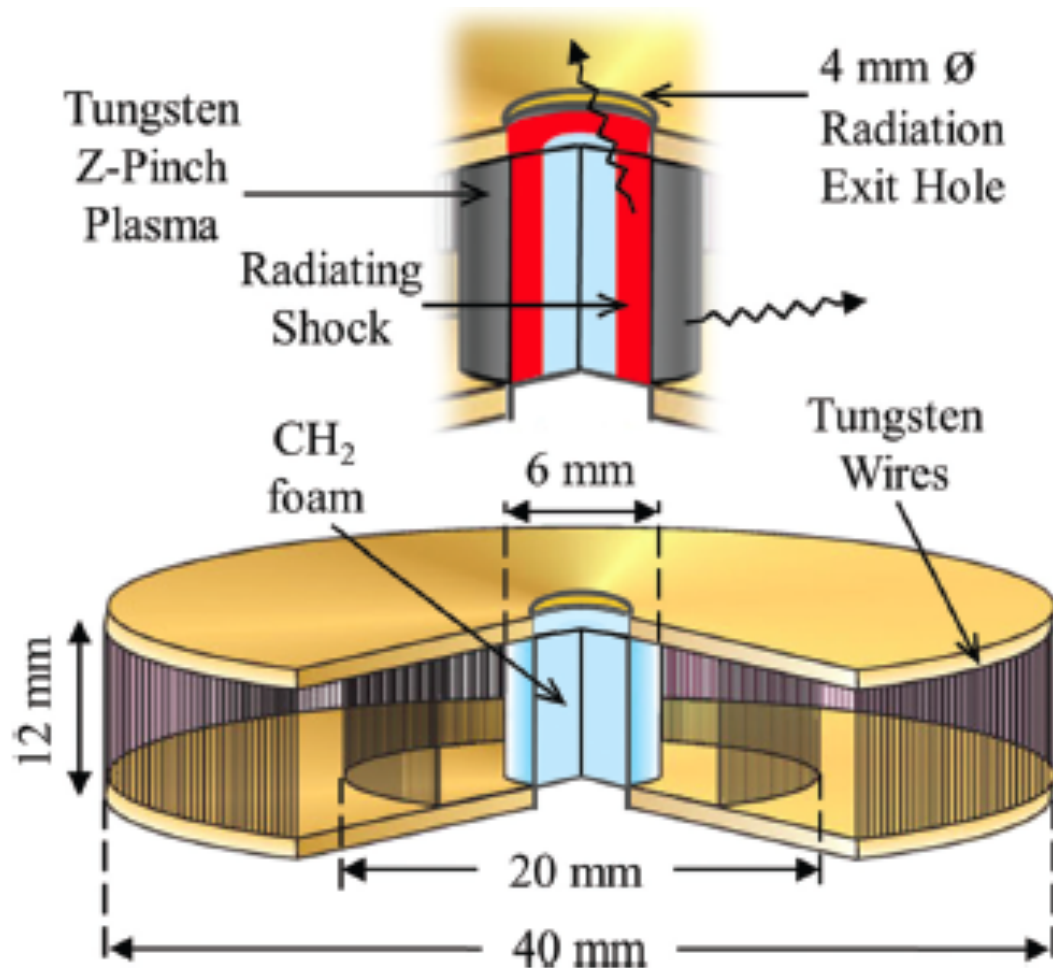
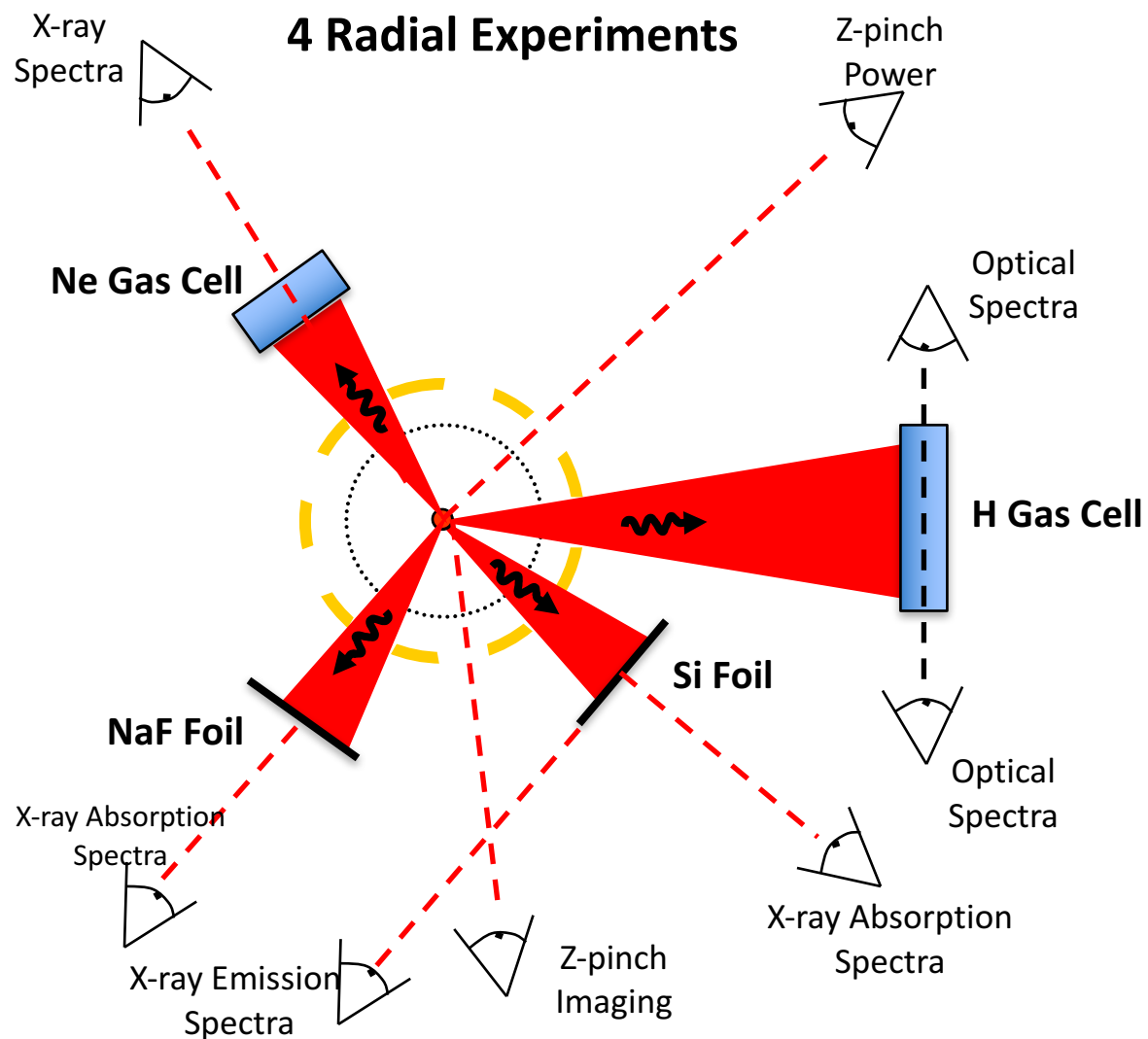
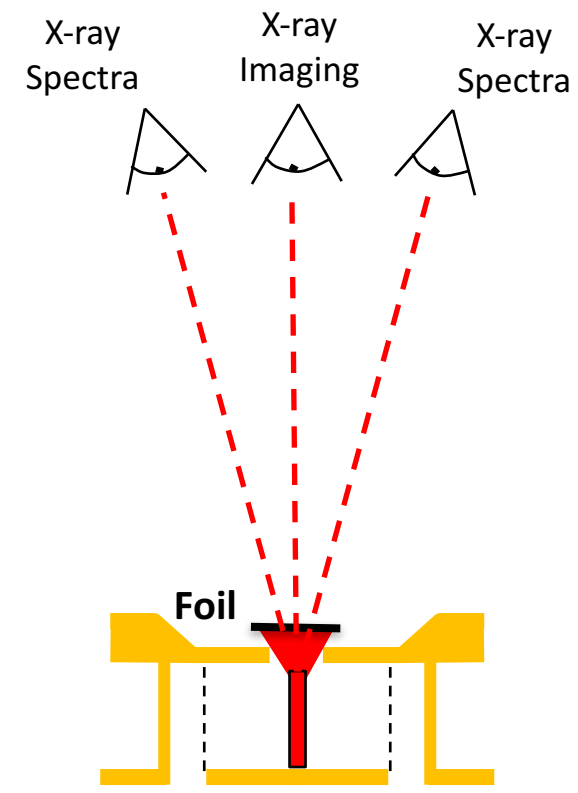


FIG. 1. Schematic of the z-pinch dynamic hohlraum. When the tungsten z pinch implodes onto the low-density CH₂ foam (inset), it launches a radiating shock emitting x-rays that escape through the axial radiation exit hole. The hot tungsten plasma radiates x-rays that escape radially.

The z-pinch x-ray source simultaneously drives 4 experiments*



1 Axial Experiment



60 spectra are typically recorded in a single shot

**Rochau et al., PoP (2014)
Either NaF or Si foil is fielded
along line of sight 130*

Conclusion: Maximize advantage of benefits and minimize effects of limitations

- Benefits

Cost effectiveness, experimental turnaround time, level of interrogation detail, extended regime accessibility, modeling confidence, whole-device interpolation capability

- Limitations

Invasive diagnostics, boundary effects, inflexible particle distribution functions, regime-accessibility cut-offs, non-ideal MHD

- Strategic work-around to compensate limitations

Whole-device interpolation approach (experiments, diagnostics, high-fidelity numerical simulations)

The End

Thank you